

SCIENTIFIC REPORTS

OPEN

Physics of Efficiency Droop in GaN:Eu Light-Emitting Diodes

Ioannis E. Fragkos¹, Volkmar Dierolf², Yasufumi Fujiwara³ & Nelson Tansu¹

The internal quantum efficiency (IQE) of an electrically-driven GaN:Eu based device for red light emission is analyzed in the framework of a current injection efficiency model (CIE). The excitation path of the Eu^{+3} ion is decomposed in a multiple level system, which includes the carrier transport phenomena across the GaN/GaN:Eu/GaN active region of the device, and the interactions among traps, Eu^{+3} ions and the GaN host. The identification and analysis of the limiting factors of the IQE are accomplished through the CIE model. The CIE model provides a guidance for high IQE in the electrically-driven GaN:Eu based red light emitters.

In recent years, the incorporation of rare-earth (RE) elements in wide bandgap semiconductors, such as gallium nitride (GaN) has opened the way for light emitters in the wavelength range of the characteristic emission of the RE ion^{1–5}. In particular, the incorporation of europium (Eu) into the GaN host (GaN:Eu) has attracted considerable attention because it enables red light emission and it has the potential to be used as an alternative to the low efficiency InGaN based red light emitters⁶. The excitation of the Eu^{+3} ion through the GaN host, results in light emission in the red spectral regime, and this has enabled the realization of GaN:Eu based devices in the last decade^{7–24}. Despite the continues improvements of the GaN:Eu devices, the external quantum efficiency (η_{EQE}) of the device exhibits a droop characteristic with increasing the current into the device^{18,21–23,25}. The droop phenomenon of the external quantum efficiency (η_{EQE}) needs to be clarified and suppressed in order to implement the GaN:Eu devices for technological applications. Therefore, the identification and understating of the limiting factors which result in the efficiency droop issue of the external quantum efficiency (η_{EQE}) is crucial for the design and realization of high efficiency GaN:Eu based devices.

It is known that the excitation of the Eu^{+3} ions in the GaN host is mediated by traps which are close to the vicinity of the Eu^{+3} ions^{8,9,21,26–29}. The injected electron-hole pairs in the GaN host are captured from these traps where they recombine and release energy. The released energy is used for the excitation of the nearby Eu^{+3} ion. The excitation path of the Eu^{+3} ion is a complex process since different carrier processes are involved, specifically including carrier transport across the GaN:Eu device, fundamental recombination processes of carriers in the GaN host, and interactions between the host, traps and Eu^{+3} ions. To the best of our knowledge, an analytical model which can describe the efficiency of the electrically-driven GaN:Eu device in the basis of the different processes and mechanisms involved in the Eu^{+3} excitation path, has not been developed until recently³⁰.

In our recent work, we developed a current injection efficiency model (CIE) both for optically-pumped and electrically-driven GaN:Eu based device with an $\text{Al}_x\text{Ga}_{1-x}\text{N}/\text{GaN:Eu}/\text{Al}_x\text{Ga}_{1-x}\text{N}$ quantum well (QW) active region³⁰. In this work, we develop a CIE model for electrically-driven GaN:Eu device with a GaN/GaN:Eu/GaN active region to identify the limiting factors of the internal quantum efficiency (η_{IQE}) and explain the efficiency droop issue of this type of active region. This type of structure is fundamentally different from the structure investigated in our previous work on quantum well based active region³⁰. The present model provides the analysis of the current injection efficiency and IQE in the structures pursued by experimentalists²³, specifically the active region with GaN/GaN:Eu where the active regions (GaN:Eu) were not confined by larger bandgap barrier systems. Such structure presented a very different challenge, which also required a completely different physics of carrier transport – beyond the QW model³⁰. This present model is important for enabling the direct comparison with the experimental devices, and providing new strategies (see Section IV) for the experimentalists to increase the IQE and suppress the droop issue in electrically-driven rare-earth doped GaN LED.

¹Center for Photonics and Nanoelectronics, Department of Electrical and Computer Engineering, Lehigh University, Bethlehem, PA, 18015, USA. ²Department of Physics, Lehigh University, Bethlehem, PA, 18015, USA. ³Division of Materials and Manufacturing Science, Graduate School of Engineering, Osaka University, Suita, Osaka, 565-0871, Japan. Correspondence and requests for materials should be addressed to I.E.F. (email: iof213@lehigh.edu) or N.T. (email: tansu@lehigh.edu)

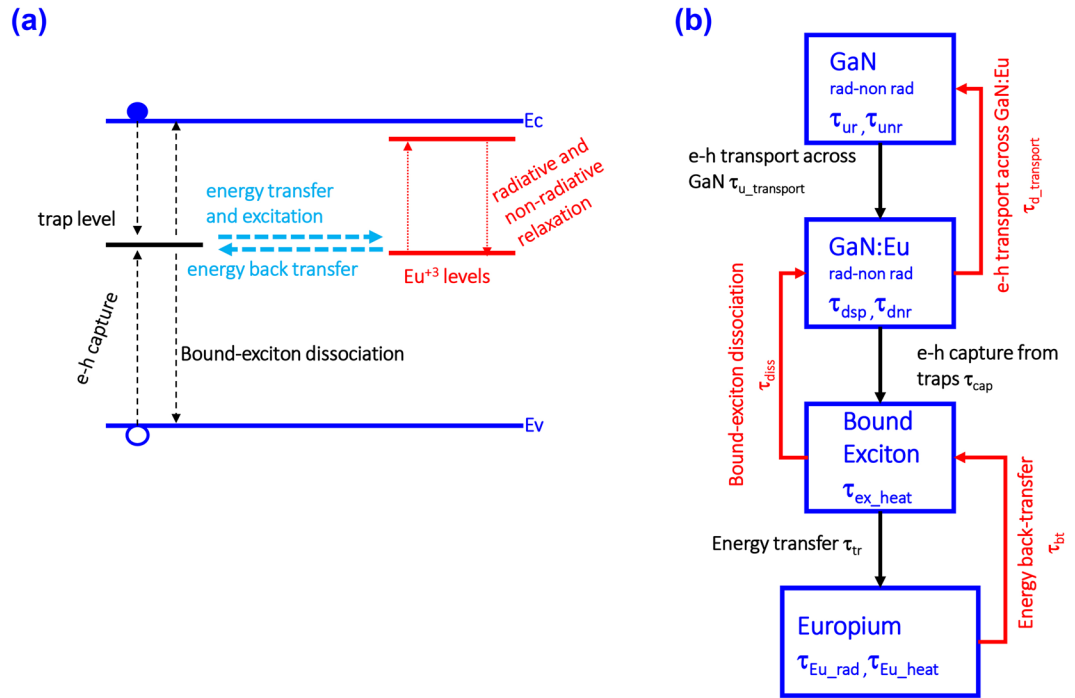


Figure 1. (a) Trap assisted excitation path of Eu^{+3} ion in the GaN host. The free electron-hole pairs present in the GaN host are captured by traps close to the vicinity of Eu^{+3} ions and form bound-excitons. The recombination of bound-excitons can result to energy transfer and excitation of a nearby Eu^{+3} ion. The excited Eu^{+3} ion can de-excite non-radiatively and radiatively as well as non-radiatively by releasing the energy to a nearby trap to form a bound-exciton. (b) Different levels and processes in the GaN/GaN:Eu/GaN active region structure. Each level includes its own related mechanisms, i.e. radiative and non-radiative recombination processes for the “GaN” and “GaN:Eu” levels (Auger, Bimolecular and Shockley-Hall-Read recombination), de-excitation process with heat release to the crystal lattice for the “Bound-Exciton” level and radiative and non-radiative processes for the “Europium” level. The individual levels are connected through the “forward mechanisms” (black-arrows) and “backward mechanisms” (red-arrows).

Current Injection Efficiency Model of the GaN:Eu active region

It is known that traps present in the vicinity of Eu^{+3} ions assist the excitation of the Eu^{+3} ion for red light emission. More specifically, studies have revealed several emission sites related to different configurations of trap- Eu^{+3} ion known as complexes^{26,28}. In our model, we simplify this picture assuming a single level trap located near to the Eu^{+3} ion.

As shown in Fig. 1(a), the free electron-hole pairs (e-h) present in the GaN host are captured by traps with a characteristic rate of $1/\tau_{\text{cap}}$. This state of captured electron-hole pairs at the trap level is denoted as bound-exciton formation in our model. The recombination of e-h pair at the trap level can result in the energy transfer and excitation to a nearby Eu^{+3} ion ($1/\tau_{\text{tr}}$). In addition, different processes can take place at the trap level, including the non-radiative recombination of e-h pairs, which results in heat transfer to the lattice ($1/\tau_{\text{ex_heat}}$), as well as the bound-exciton dissociation process which leads to the release of the electron and hole back to the conduction band and valence band respectively ($1/\tau_{\text{diss}}$). The de-excitation process of the Eu^{+3} ion consists of the radiative ($1/\tau_{\text{rad}}$) and non-radiative ($1/\tau_{\text{Eu_heat}}$) processes, as well as the energy back-transfer process resulting in a formation of a bound-exciton ($1/\tau_{\text{bt}}$).

Figure 1(b) depicts the GaN/GaN:Eu/GaN active region structure and the related carrier mechanisms along the Eu^{+3} excitation path. According to our model, radiative and non-radiative recombination processes of carriers exist both in GaN and GaN:Eu regions. These fundamental processes are described through the Auger and the Shockley-Hall-Read (SHR) recombination processes (non-radiative) and the bimolecular recombination process (radiative) in the semiconductors. In addition, carrier transport mechanisms across the structure are present which are described through the ambipolar diffusion carrier transport across the GaN and GaN:Eu regions^{31–34}.

The development of the current injection efficiency model for the GaN:Eu/GaN based LED is developed here, and the framework follows the treatments presented for III-V^{31,32} and GaN-based³³ lasers/LEDs. The rate equations of carriers in the GaN region (N_1) and GaN:Eu region (N_2) are given by:

$$\frac{dN_1}{dt} = \frac{I_{\text{tot}}}{q V_1} + \frac{N_2}{\tau_{r2}} \frac{V_2}{V_1} - N_1 \left(\frac{1}{\tau_{nr1}} + \frac{1}{\tau_{sp1}} + \frac{1}{\tau_{r1}} \right), \quad (1)$$

$$\frac{dN_2}{dt} = \frac{N_1}{\tau_{r1}} \frac{V_1}{V_2} + \frac{N_{ex}}{\tau_{diss}} - N_2 \left(\frac{1}{\tau_{nr2}} + \frac{1}{\tau_{sp2}} + \frac{1}{\tau_{r2}} + \frac{1}{\tau_{cap}} \right), \quad (2)$$

with the rate $1/\tau_{cap}$ defined as

$$\frac{1}{\tau_{cap}} = \frac{1}{\tau_{cap0}} \left(1 - \frac{N_{ex}}{N_{traps}} \right). \quad (3)$$

The I_{tot} is the total current injected into the GaN region from the n- and p-cladding layers of device. The parameters, N_{ex} and N_{traps} , denote the bound-excitons and the maximum available trap concentration in the GaN:Eu region, respectively, and the τ_{cap0} is the capture time at the low regime where $N_{ex} \ll N_{traps}$. In equations (1) and (2), the V_1 and V_2 are the volumes of the GaN and GaN:Eu regions respectively. The rates $1/\tau_{nr1}$, $1/\tau_{sp1}$, $1/\tau_{nr2}$ and $1/\tau_{sp2}$ are the non-radiative and spontaneous radiative recombination rates in the GaN (subscript 1) and GaN:Eu (subscript 2) regions, respectively. These rates are described by the SHR recombination constants A, the Auger coefficient C, and the bimolecular recombination constant B in the semiconductors. The rates $1/\tau_{r1}$ and $1/\tau_{r2}$ are described by the ambipolar diffusion carrier transport time in the GaN and GaN:Eu regions respectively.

The rate equations of bound-excitons and excited Eu^{+3} ion concentration are given by:

$$\frac{dN_{ex}}{dt} = N_2 \frac{1}{\tau_{cap}} + N_{Eu} \frac{1}{\tau_{bt}} - N_{ex} \left(\frac{1}{\tau_{tr}} + \frac{1}{\tau_{diss}} + \frac{1}{\tau_{ex,heat}} \right), \quad (4)$$

$$\frac{dN_{Eu}}{dt} = N_{ex} \frac{1}{\tau_{tr}} - N_{Eu} \left(\frac{1}{\tau_{bt}} + \frac{1}{\tau_{rad}} + \frac{1}{\tau_{Eu,heat}} \right), \quad (5)$$

The rates $1/\tau_{tr}$ and $1/\tau_{bt}$ are defined in an equivalent manner as in equation (3):

$$\frac{1}{\tau_{tr}} = \frac{1}{\tau_{tr0}} \left(1 - \frac{N_{Eu}}{N} \right), \quad (6)$$

$$\frac{1}{\tau_{bt}} = \frac{1}{\tau_{bt0}} \left(1 - \frac{N_{ex}}{N_{traps}} \right), \quad (7)$$

where the N_{Eu} and N are the excited and the maximum concentrations of Eu^{+3} ions in the GaN:Eu region, respectively.

The current injection efficiency ($\eta_{injection}$) is defined as the ratio of the current arising from the radiative and non-radiative de-excitation of Eu^{+3} ions over the total current I_{tot} , entering the device:

$$\eta_{injection} = \frac{I_{Eu}}{I_{tot}}. \quad (8)$$

The I_{Eu} corresponds to the total recombination current arising from the radiative and non-radiative de-excitation of the Eu^{+3} ion in the GaN:Eu region:

$$I_{Eu} = \frac{N_{Eu} q V_{Eu}}{\tau}, \quad (9)$$

with q as the electron charge, and the lifetime has both contributions from the radiative and non-radiative processes as stated below:

$$\frac{1}{\tau} = \frac{1}{\tau_{rad}} + \frac{1}{\tau_{Eu,heat}}, \quad (10)$$

By solving the rate equations (1), (2), (4), and (5) under steady state conditions and using the equation (8), the current injection efficiency for the GaN:Eu / GaN LED can be expressed as:

$$\eta_{injection} = \left[\left(\frac{L_1}{L_2} \right) \left(b + \frac{b}{\left(\frac{1}{\tau_{r1}} + \frac{1}{\tau_{sp1}} + \frac{1}{\tau_{nr1}} \right)^{-1}} - \left(\frac{L_2}{L_1} \right) \frac{c}{\tau_{r2}} \right) \right]^{-1} \quad (11)$$

with

Parameters	Study I	Study II	Study III	Study V	Study VI	Study VII
A (10^8 s^{-1})	0.001–1	0.1	0.1	0.1	0.1	0.1
$\tau_{\text{cap}0}$ (10^{-8} s)	100	100	1–1000	100	100	100
$\tau_{\text{tr}0}$ (10^{-7} s)	360	360	360	0.36–3600	360	360
τ_{diss} (10^{-6} s)	1000	1000	1000	1000	1000	1000
$\tau_{\text{bt}0}$ (10^{-6} s)	200	200	200	200	200	200
$\tau_{\text{ex,heat}}$ (10^{-3} s)	1	1	1	1	1	1
$\tau_{\text{Eu,heat}}$ (10^{-3} s)	1	1	1	1	1	1
τ_{rad} (10^{-6} s)	400	400	400	400	10–600	400
N (10^{19} cm^{-3})	1	1	1	1	0.1–10	0.1–10
$N_{\text{traps}}^{\dagger}$ (10^{19} cm^{-3})	1	1	1	1	0.1–10	0.1–10
$L_{\text{GaN}}, L_{\text{GaN:Eu}}$ (nm)	5, 2.5	2.5–6.5, 2.5–6.5	5, 2.5	5, 2.5	5, 2.5	QW region

Table 1. Parameters used for the numerical calculations.

$$b = \frac{L_2}{L_1} \left(a - \frac{\left(\frac{1}{\tau_{\text{rad}}} + \frac{1}{\tau_{\text{Eu,heat}}} \right)^{-1} \tau_{\text{tr}}}{\left(\frac{1}{\tau_{\text{rad}}} + \frac{1}{\tau_{\text{Eu,heat}}} + \frac{1}{\tau_{\text{bt}}} \right)^{-1} \tau_{\text{diss}}} \right) \tau_{\text{tr}1} \quad (12)$$

$$a = \left(\frac{c}{\left(\frac{1}{\tau_{\text{r}2}} + \frac{1}{\tau_{\text{sp}2}} + \frac{1}{\tau_{\text{nr}2}} + \frac{1}{\tau_{\text{cap}}} \right)^{-1}} \right) \quad (13)$$

$$c = \left(\left(\frac{\left(\frac{1}{\tau_{\text{rad}}} + \frac{1}{\tau_{\text{Eu,heat}}} \right)^{-1} \tau_{\text{tr}}}{\left(\frac{1}{\tau_{\text{rad}}} + \frac{1}{\tau_{\text{Eu,heat}}} + \frac{1}{\tau_{\text{bt}}} \right)^{-1} \tau_{\text{diss}}} - \frac{\left(\frac{1}{\tau_{\text{rad}}} + \frac{1}{\tau_{\text{Eu,heat}}} \right)^{-1}}{\tau_{\text{bt}}} \right) \tau_{\text{cap}} \right) \quad (14)$$

where, the L_1 and L_2 are the lengths of the GaN and GaN:Eu regions respectively. Then, the internal quantum efficiency (η_{IQE}) of the rare-earth doped GaN LED is given by:

$$\eta_{\text{IQE}} = \eta_{\text{injection}} \cdot \eta_{\text{rad}} \quad (15)$$

where, the η_{rad} is the radiative efficiency of the Eu^{+3} ions defined as the ratio of radiative to both radiative and non-radiative de-excitation of Eu^{+3} ions:

$$\eta_{\text{rad}} = \frac{N_{\text{Eu}}/\tau_{\text{rad}}}{N_{\text{Eu}}/\tau} = \frac{1}{\frac{1}{\tau_{\text{rad}}} + \frac{1}{\tau_{\text{Eu,heat}}}} \quad (16)$$

Simulation Results

Table 1 summarizes the parameters used for each numerical calculation. The material parameters used for the simulations, such as SHR recombination constant A, bimolecular recombination constant B, Auger coefficient C, electron and hole effective masses and mobilities can be found in ref.³³. For this work we assume the same values of material parameters both for the GaN and GaN:Eu region. In addition, for the magnitude of the relative times related to traps, bound-excitons and Eu^{+3} ions, the experimental results described in^{35,36} were used as a point of reference.

For each study, the current injection efficiency ($\eta_{\text{injection}}$) and the excited Eu^{+3} ion concentration are plotted versus the current density J entering the GaN:Eu device. From our studies, the current injection efficiencies ($\eta_{\text{injection}}$) of the GaN:Eu LEDs exhibit the drooping characteristics with increasing current density J . This droop characteristic, which is present in the case studies, arises from the saturation of the excited Eu^{+3} ions in the active region. The excited Eu^{+3} ion concentration cannot exceed the maximum available concentration (N) in the GaN:Eu region. Therefore, further increasing the injected current density into the device result in a bottleneck in the energy transfer from bound-excitons into the Eu^{+3} ions, which decreases the current injection efficiency ($\eta_{\text{injection}}$). It is important to note that the rate of this saturation and the subsequent droop in the current injection efficiency ($\eta_{\text{injection}}$) are strongly dependent on the different parameters of the Eu^{+3} excitation path. It is essential to point out that the effect of Auger recombination in our studies is expected to be negligible due to the relatively low carrier concentration of $\sim 10^{18} \text{ cm}^{-3}$ in the active region for electrically-driven GaN:Eu LEDs ($J \sim 10 \text{ A/cm}^2$).

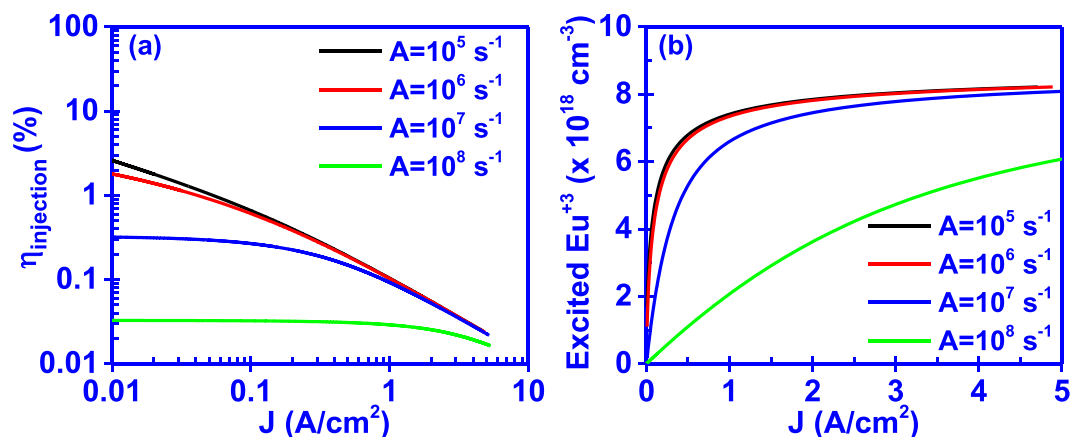


Figure 2. Effect of Shockley-Hall-Read constant A on the (a) current injection efficiency ($\eta_{\text{injection}}$) and (b) excited Eu^{+3} ion concentration of the GaN:Eu active region.

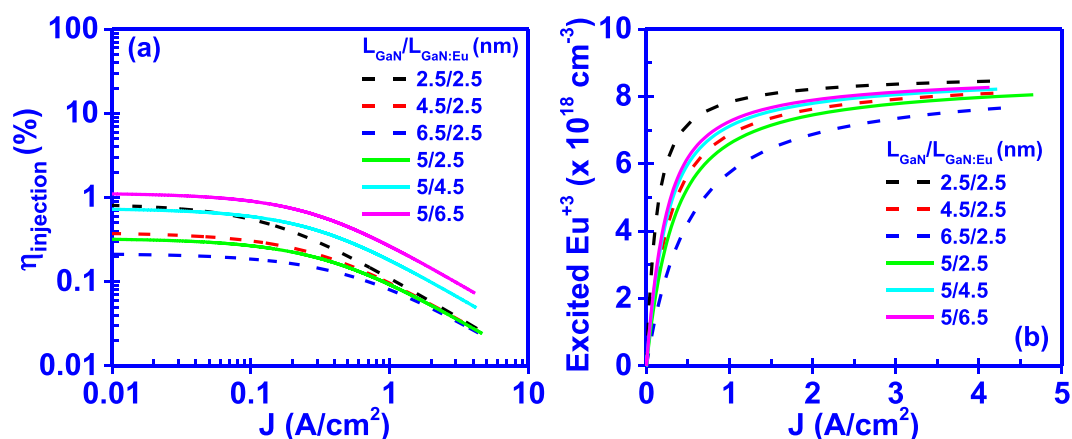


Figure 3. Effect of GaN and GaN:Eu region lengths ($L_{\text{GaN}}/L_{\text{GaN:Eu}}$) on (a) current injection efficiency ($\eta_{\text{injection}}$) and (b) excited Eu^{+3} ion concentration of the GaN:Eu region. The dashed lines correspond to changes in the length of the GaN region (L_{GaN}) with a fixed $L_{\text{GaN:Eu}} = 2.5 \text{ nm}$. Similarly, the solid lines corresponds to changes in the length of the GaN:Eu region ($L_{\text{GaN:Eu}}$) with a fixed $L_{\text{GaN}} = 5 \text{ nm}$.

Effect of Shockley-Hall-Read constant A . The Shockley-Hall-Read constant A (SHR), is related to defects which are present in the crystal lattice and are not related to the incorporation of the Eu^{+3} ions in the GaN host, thus do not assist the Eu^{+3} excitation. However, they capture free carriers and contribute to the non-radiative recombination process. As shown in Fig. 2a and b, decreasing the SHR constant A results in higher current injection efficiencies ($\eta_{\text{injection}}$) as well as in faster saturation rates of the excited Eu^{+3} ion concentration. The low values of A indicate lower non-radiative recombination rates of carriers, thus more carriers are available to contribute to the excitation of Eu^{+3} ions. Furthermore, decreasing the A below $A=10^6 \text{ s}^{-1}$, results in a minimal effect on the current injection efficiency ($\eta_{\text{injection}}$) and excited Eu^{+3} ion concentration for the given range of input current densities J of the device.

Effect of GaN and GaN:Eu region lengths. The effect of the lengths of the GaN and GaN:Eu regions is depicted in Fig. 3. As it is shown, the increase of the GaN length (L_{GaN}) reduces the current injection efficiency ($\eta_{\text{injection}}$) and excited Eu^{+3} ion concentration. In contrast, an increase in the GaN:Eu length ($L_{\text{GaN:Eu}}$) will give rise to the current injection efficiency ($\eta_{\text{injection}}$) as well as to the excited Eu^{+3} ion concentration under steady state conditions. The change in the lengths of the two regions affects the ambipolar diffusion transport time (τ_{r1} , τ_{r2}) of carriers across the structure. For higher L_{GaN} , the carriers require more time to be transported across the GaN region, reducing the rate at which they arrive in the GaN:Eu region. As a result, the current injection efficiency ($\eta_{\text{injection}}$) and excited Eu^{+3} ion concentration in the active region are decreased. In contrast, for higher $L_{\text{GaN:Eu}}$, the ambipolar diffusion transport time in the GaN:Eu region (τ_{r2}) will be increased giving rise to the carrier concentration in the GaN:Eu region. The increased carrier concentration in the GaN:Eu region will result in higher probability of bound-exciton formation. Consequently, the excited Eu^{+3} ion concentration and the current injection efficiency ($\eta_{\text{injection}}$) are increased.

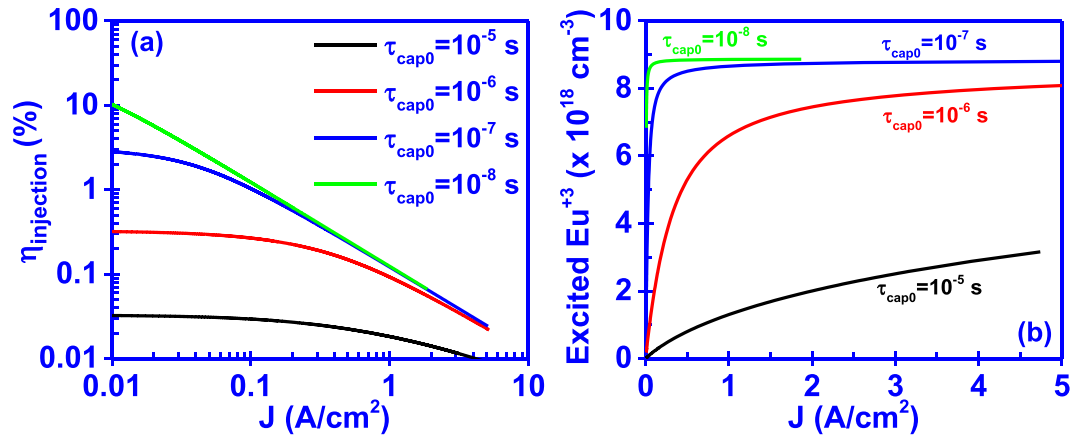


Figure 4. Effect of capture time ($\tau_{\text{cap}0}$) on the (a) current injection efficiency ($\eta_{\text{injection}}$) and (b) excited Eu^{+3} ion concentration of the GaN:Eu active region.

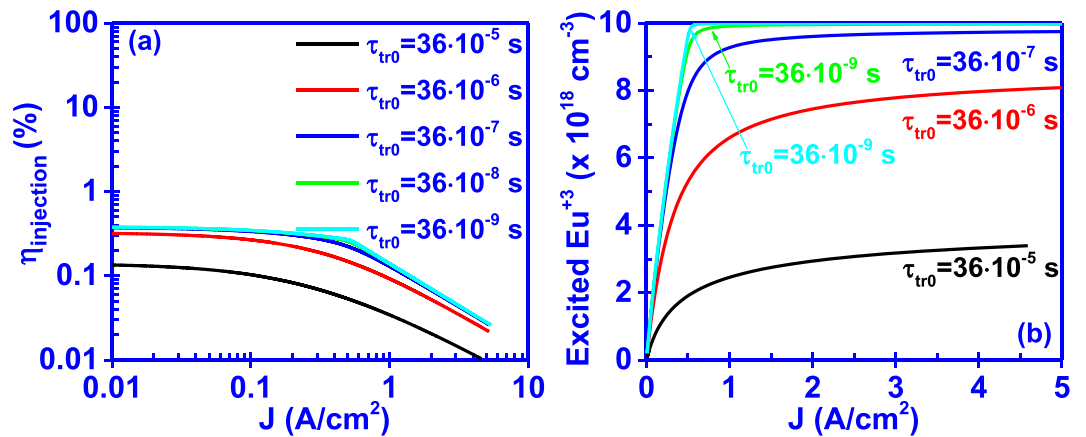


Figure 5. Effect of transfer time ($\tau_{\text{tr}0}$) on the (a) current injection efficiency ($\eta_{\text{injection}}$) and (b) excited Eu^{+3} ion concentration of the GaN:Eu active region.

Effect of capture time. The capture time from traps ($\tau_{\text{cap}0}$), which are associated with the incorporation of Eu^{+3} ions, defines the rate at which bound-excitons are formed by capturing e-h pairs from the GaN host. It is clearly seen from Fig. 4a and b that decreasing the capture time, the current injection efficiency ($\eta_{\text{injection}}$) increases while the Eu^{+3} ion concentration saturates faster. From equation (4), the lower capture time results in a higher formation rate of bound-excitons which in turn gives rise to the excitation rate of Eu^{+3} ions under steady state conditions.

In addition, for the cases with capture times lower than $\tau_{\text{cap}0} = 10^{-7}$ s, the changes in the current injection efficiency ($\eta_{\text{injection}}$) are prominent at low current densities, which can be attributed to the faster saturation of the excited Eu^{+3} ion concentration. Despite the faster capture rate $\tau_{\text{cap}0}$ of carriers from traps, the saturation of the excited Eu^{+3} ion will remain the bottleneck in the injection process in high current density regime.

Effect of transfer time. The excitation process of the Eu^{+3} ions is driven by the energy transfer from the bound-excitons formed by the captured e-h pairs in the traps. This transfer rate ($1/\tau_{\text{tr}0}$) is dictated by the strength of the interaction between the bound-excitons and Eu^{+3} ions. Figure 5a and b depict the effect of the transfer time in the current injection efficiency ($\eta_{\text{injection}}$) and excited Eu^{+3} ion concentration, respectively. As the transfer time decreases, the current injection efficiency ($\eta_{\text{injection}}$) increases accompanied by the higher saturation of the excited Eu^{+3} ion up to higher current density level. However, a decrease of transfer time below $\tau_{\text{tr}0} = 36 \times 10^{-7}$ s does not have a significant effect on the current injection efficiency ($\eta_{\text{injection}}$) since the excited Eu^{+3} ion concentration remains almost unaffected under further reduction of the transfer time ($\tau_{\text{tr}0}$).

Effect of radiative lifetime of Eu^{+3} ion. The changes in the trap capture, transport, transfer, and recombination rates – as discussed above – show the ability to engineer the current injection efficiency in RE-doped GaN LEDs at the low injection current density level. The optimized structure – based on the results above – enables up

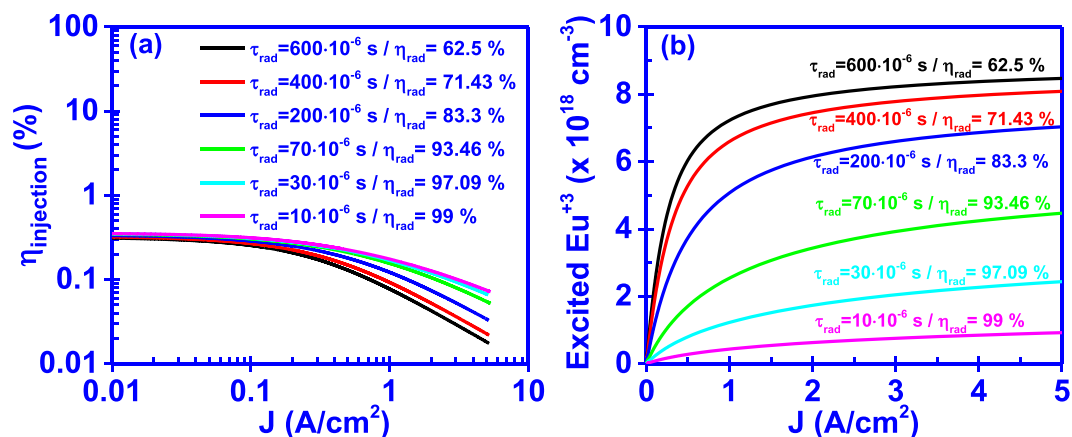


Figure 6. Effect of radiative lifetime of Eu^{+3} ion (τ_{rad}) on the (a) current injection efficiency ($\eta_{\text{injection}}$) and (b) excited Eu^{+3} ion concentration of the GaN:Eu active region. Each radiative lifetime results in different radiative efficiency of the excited Eu^{+3} ions.

to $\eta_{\text{injection}} \sim 10\%$ at low injection current density level, while our finding shows that the engineering of the radiative lifetime for the RE-ions will be instrumental in governing the current injection efficiency properties at high current density level.

To alter the current injection efficiency ($\eta_{\text{injection}}$) at higher input current densities it is necessary to delay the saturation of Eu^{+3} ions. This can be accomplished by reducing the radiative lifetime of Eu^{+3} ions (τ_{rad}). From equations (9) and (10) the lower radiative lifetime (τ_{rad}) of Eu^{+3} ions will increase the radiative recombination rate and also the current injection efficiency ($\eta_{\text{injection}}$) at a particular input current. Furthermore, the radiative efficiency (η_{rad}) of the system will be increased, giving additional rise to the internal quantum efficiency (η_{IQE}) of the active region.

As shown in Fig. 6a and b, reducing the radiative lifetime (τ_{rad}) of Eu^{+3} ions results in the increased current injection efficiency ($\eta_{\text{injection}}$) at higher input current densities. This arises from the lower saturation values of excited Eu^{+3} ions at the given input current density range, as shown in Fig. 6(b). A change of the radiative lifetime from $\tau_{\text{rad}} = 600 \mu\text{s}$ to $\tau_{\text{rad}} = 10 \mu\text{s}$, at a current density of $J = 4 \text{ A}/\text{cm}^2$, will result in an increase of 214% in the current injection efficiency ($\eta_{\text{injection}}$) and in a reduction of 90% in the excited of Eu^{+3} ion concentration in the active region.

Effect of carrier confinement in the GaN:Eu region. The utilization of heterostructures such as $\text{Al}_x\text{Ga}_{1-x}\text{N}/\text{GaN:Eu}/\text{Al}_x\text{Ga}_{1-x}\text{N}$ increases the carrier confinement in the GaN:Eu quantum well (QW) region³⁰, enhancing in that way the excitation probability of Eu^{+3} ions. In addition, the replacement of the GaN/GaN:Eu/GaN structure with the $\text{Al}_x\text{Ga}_{1-x}\text{N}/\text{GaN:Eu}/\text{Al}_x\text{Ga}_{1-x}\text{N}$ heterostructure results in different carrier processes (Fig. 7). These additional processes include the quantum mechanical capture process of carriers from the barrier to the QW and the thermionic carrier escape process from the GaN:Eu QW to the $\text{Al}_x\text{Ga}_{1-x}\text{N}$ barriers.

The effect of the carrier confinement on the current injection process in RE-doped GaN LED is shown in Fig. 8. The presence of the GaN:Eu quantum well (QW) confined within $\text{Al}_x\text{Ga}_{1-x}\text{N}$ barriers increases the current injection efficiency ($\eta_{\text{injection}}$) and the excited Eu^{+3} ion concentration at a given current density. The carrier confinement in the QW increases the carrier density near the Eu^{+3} ions and thus, the probability of carrier capture from traps increases, giving rise to the excitation of Eu^{+3} ions. In addition, increasing the Al composition of the $\text{Al}_x\text{Ga}_{1-x}\text{N}$ barrier increases the barrier height, which results in the suppression of the thermionic carrier escape process³³. As a result, the current injection efficiency ($\eta_{\text{injection}}$) and excited Eu^{+3} ion concentration in the active region are increased. The effect of carrier confinement, has been demonstrated by T. Arai *et al.*²¹, where they showed an increase of the PL intensity of a AlGaIn/GaN:Eu/AlGaIn multiple QW structure as compared to a rudimentary GaN:Eu based light emitter. Similar findings have been demonstrated for Erbium-doped GaN based heterostructures, where the effect of carrier confinement increases the luminescence of the GaN:Er emitter^{37,38}.

DroopSuppressions

Based on our analysis, we present several experimental pathways on how to increase the internal quantum efficiency (η_{IQE}) of the GaN:Eu based devices, including strategies for suppressing droop. In Fig. 9, the internal quantum efficiency (η_{IQE}) is decomposed into two components, namely the current injection ($\eta_{\text{injection}}$) and radiative (η_{rad}) efficiencies. The individual efficiencies depend on specific phenomena along the excitation path of Eu^{+3} ions. The experimental pathway on how to alter these phenomena, in favor of the respective efficiency, are also shown in Fig. 9.

The utilization of advanced growth techniques such as metalorganic chemical vapor deposition technique (MOCVD) can result in high crystal quality^{39–42}. By carefully adjusting the growth parameters, the defect concentration in the GaN host can be minimized resulting in lower SHR recombination constant A. In addition, the lower defect concentration will give rise to the carrier mobility along the structure due to reduction of the scattering centers. The carrier mobility affects the transport time, which plays an essential

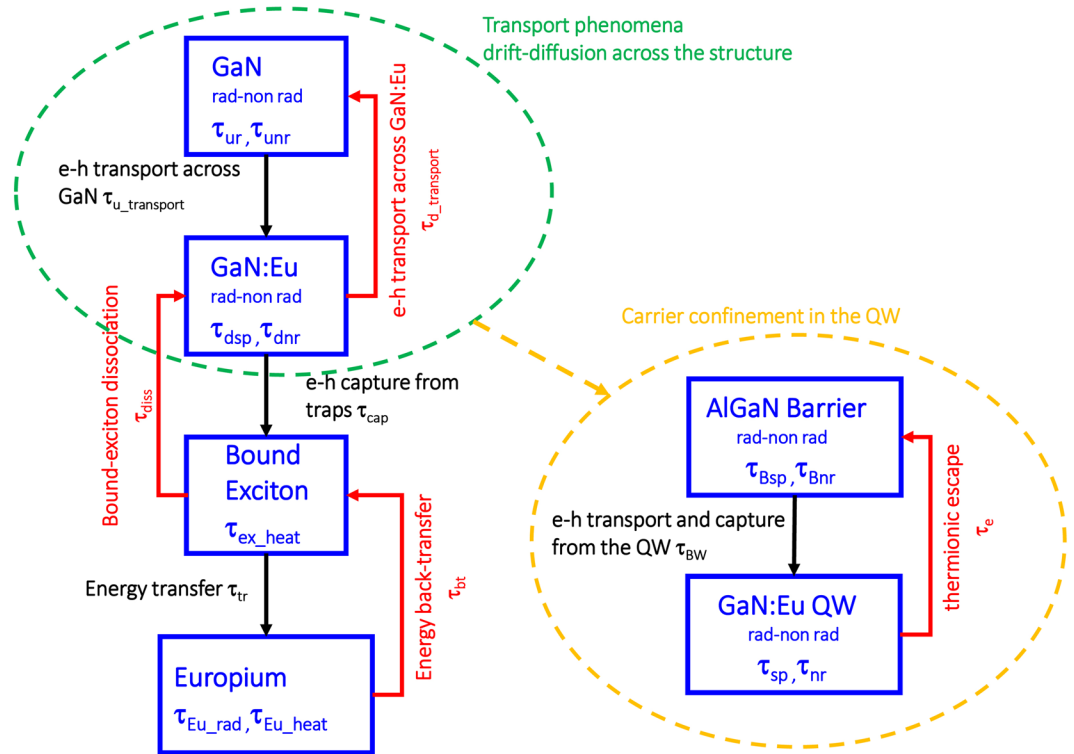


Figure 7. Active region structures for a GaN:eu based device. The effect of the $\text{Al}_x\text{Ga}_{1-x}\text{N}/\text{GaN:Eu}/\text{Al}_x\text{Ga}_{1-x}\text{N}$ heterostructure results in the formation of a GaN:Eu quantum well (QW). This QW structure results in quantum mechanical processes such as the capture of carriers from the barrier to the QW as well as to the thermionic carrier escape from the QW to the barrier. The carrier confinement give rise to the carrier concentration inside the GaN:Eu QW which in turns enhances the excitation probability of Eu^{+3} ions.

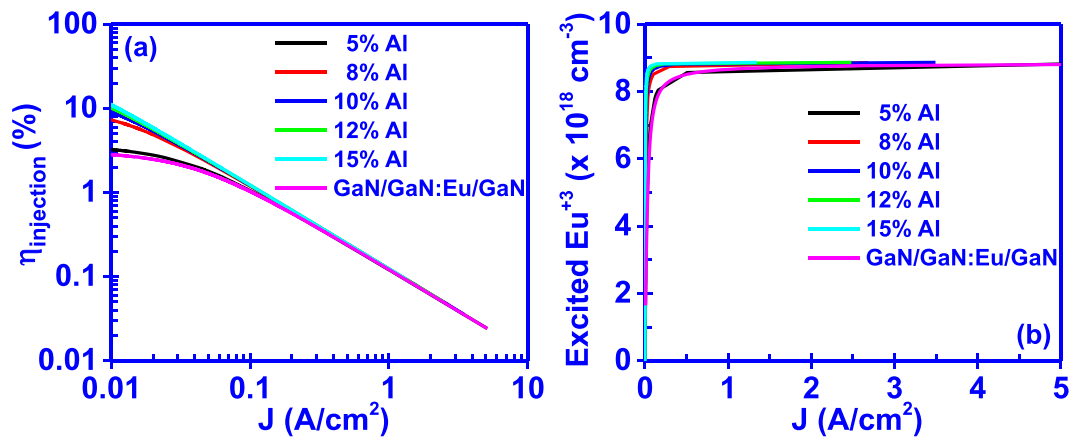


Figure 8. Effect of carrier confinement on (a) current injection efficiency ($\eta_{\text{injection}}$) and (b) excited Eu^{+3} ion concentration of the GaN:Eu active region. Higher Al percentage in the $\text{Al}_x\text{Ga}_{1-x}\text{N}$ barrier results in the suppression of the thermionic emission of carriers from the GaN:Eu QW to the $\text{Al}_x\text{Ga}_{1-x}\text{N}$ barrier.

role in the electrically-driven internal quantum efficiency (η_{IQE}) of the system. The direct effect of carrier mobility was not presented here, but it is evident through the ambipolar diffusion transport time^{31–34}. For higher carrier mobility in the GaN region, the current injection efficiency ($\eta_{\text{injection}}$) will be enhanced in the RE-doped LEDs. In contrast, the higher carrier mobility in the GaN:Eu region will result in lower current injection efficiency ($\eta_{\text{injection}}$) and lower excited Eu^{+3} ion concentration in the active region. Both the carrier mobility and length of the device active regions affect the transport time. Furthermore, the utilization of heterostructure will be beneficial for the internal quantum efficiency (η_{IQE}), attributed to the stronger carrier localization which in turn increases the trap capture probabilities^{21,37,38}. In order to obtain a more efficient excitation of Eu^{+3} ion, co-doping and strain engineering in the GaN host are possible pathways.

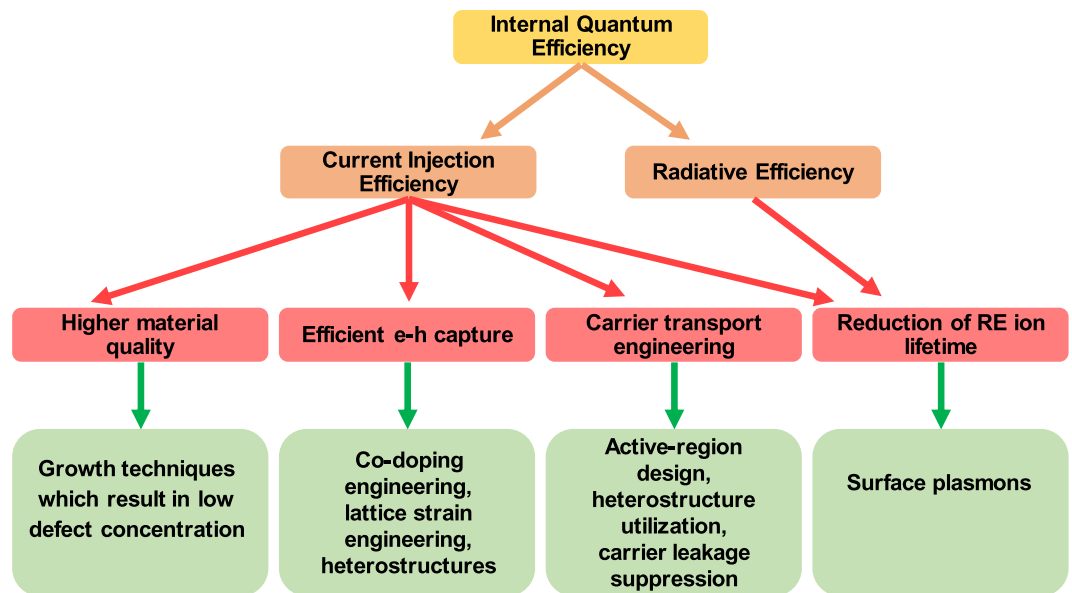


Figure 9. Internal Quantum Efficiency in the GaN:Eu based devices and its dependency on the parameters along the excitation path of Eu^{+3} ion.

These methods have been proved to result in more efficient capture process and energy transfer process to the Eu^{+3} ion^{18,23,25,26,28,29,43}.

The effect of radiative lifetime of Eu^{+3} ions is crucial for the internal quantum efficiency (η_{IQE}) of the device. From our analysis, the current injection efficiency ($\eta_{\text{injection}}$) and consequently the internal quantum efficiency (η_{IQE}) are limited by the saturation of the excited Eu^{+3} ion concentration at higher input current densities. In order to achieve higher efficiencies at higher input current densities, the change of this saturation rate is essential. It has been experimentally demonstrated that by utilizing surface-plasmon (SP) in GaN-based QW can significantly increase the radiative efficiency of the system^{44–47}. For the case of GaN:Eu based emitters, through the engineering of the deposited materials used as SPs, the SP frequency can be adjusted to be very closed to the frequency of the emitted photons from the Eu^{+3} ions. This approach will increase both the current injection efficiency ($\eta_{\text{injection}}$) and also the radiative efficiency (η_{rad}) of the system.

Comparison with experiment

The results from our CIE model are compared with the experimentally reported values. More specifically, we calculated the external quantum efficiency (η_{EQE}) of a GaN/GaN:Eu/GaN structure. The external quantum efficiency (η_{EQE}) is defined as the product of the internal quantum efficiency (η_{IQE}) and the extraction efficiency (η_{EXT}) of the device. For the purpose of these calculations, a device area of $0.1 \times 0.1 \text{ cm}^2$ with an external quantum efficiency of $\eta_{\text{EXT}} = 44\%$ was used, which is a typical value of the GaN:Eu based devices²². W. Zhu and co-workers fabricated a high power GaN:Eu based LED via low temperature MOCVD technique²³. The active region of this device consisted of alternate GaN (6 nm) and GaN:Eu (3 nm) regions and exhibited an external quantum efficiency of $\eta_{\text{EQE}} = 4.6\%$ at an injected current of 1 mA which was reduced to $\eta_{\text{EQE}} = 0.9\%$ at 20 mA. These values correspond to the highest reported external quantum efficiencies (η_{EQE}) for a GaN:Eu based device up to date.

Figure 10 presents our numerical fitting results to the experimentally reported values from W. Zhu *et al.*²³. The simulation parameters used here are presented in Table 2. Our simulated results provided an excellent fit with the experimental data from ref.²³, as shown in Fig. 10.

In order to guide the experiments, we investigated two cases (Case I and Case II) with different design parameters. In Case I (Fig. 10), by increasing the length of the GaN:Eu region from 3 nm to 6 nm, an increase of the external quantum efficiency (η_{EQE}) with respect to the fitting of the experimental data is possible. More specifically, an increase of 167%, 112% and 103% at an injected current of 5 mA, 15 mA and 30 mA respectively, is predicted. In Case II, by an additional decrease of the radiative lifetime of Eu^{+3} ion from $\tau_{\text{rad}} = 100 \mu\text{s}$ to $\tau_{\text{rad}} = 70 \mu\text{s}$, an increase of 173% and 183% at 15 mA and 30 mA respectively, is possible.

The experimental work by W. Zhu *et al.*, showed that increasing the current into the GaN:Eu device, will eventually result in the saturation of the output light power of the device, as well as, in the decrease of the external quantum efficiency (η_{EQE}). The saturation in the output power is a result of the saturation of the excited Eu^{+3} ions in the active region. Our work has showed this saturation causes the efficiency droop issue in the GaN:Eu devices. Similar results have been experimentally verified elsewhere^{18,19,21}.

Conclusion

In summary, we developed a current injection efficiency model (CIE) for a GaN:Eu based device with a GaN/GaN:Eu/GaN structure as an active region, in order to identify the limiting factors of the internal quantum efficiency (η_{IQE}) of the GaN:Eu based device. The analysis of the internal quantum efficiency (η_{IQE}) is accomplished in the basis of a multilevel system, which includes the carrier behavior and mechanisms in the GaN and GaN:Eu

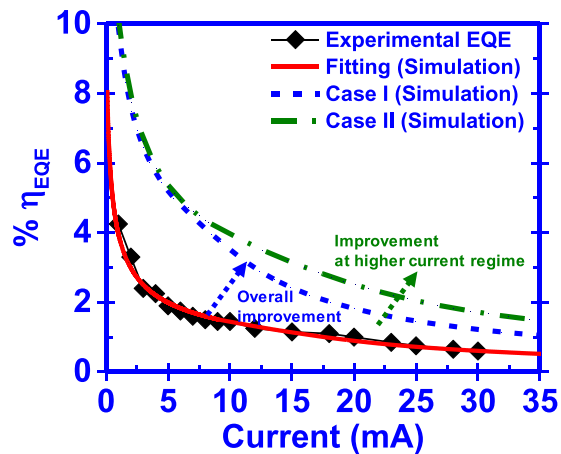


Figure 10. Experimentally reported values for a GaN:Eu device and the fitting with the CIE model. Two simulations for higher external quantum efficiency are performed. The corresponding percentage increase at the particular current, is calculated with respect to the fitting of the experimental values.

Parameters	Fitting	Case I	Case II
A (10^8 s^{-1})	0.01	0.01	0.01
τ_{cap0} (10^{-8} s)	10	10	10
τ_{tr0} (10^{-7} s)	0.36	0.36	0.36
τ_{dis} (10^{-6} s)	1000	1000	1000
τ_{bt0} (10^{-6} s)	200	200	200
$\tau_{\text{c_heat}}$ (10^{-3} s)	1	1	1
$\tau_{\text{Eu_heat}}$ (10^{-3} s)	1	1	1
τ_{rad} (10^{-6} s)	100	100	70
N (10^{19} cm^{-3})	8.7	8.7	8.7
N _{traps} (10^{19} cm^{-3})	8.7	8.7	8.7
L _{GaN} , L _{GaN:Eu} (nm)	6, 3	6, 6	6, 6

Table 2. Parameters used for the fitting of the experimental values of the GaN:Eu device and the simulations for higher external quantum efficiency (η_{EQE}).

regions and the interactions of the traps, carriers and Eu^{+3} ions with the host. It was found that the droop in the efficiency of the GaN:Eu device is associated with the droop in the current injection efficiency ($\eta_{\text{injection}}$) of the active region which arises from the saturation of the excited Eu^{+3} ion concentration in the active region. Through the manipulation of the characteristic rates and processes associated with the excitation path of Eu^{+3} ions, efficiencies higher than the current state of the art can be achieved. Our work demonstrates the pathway for enhancing the efficiency of the GaN:Eu based red light emitting devices. The CIE model can be extended to other RE-doped wide bandgap semiconductors, in which the excitation of RE ion is trap assisted.

References

- Steckl, J., Garter, M., Lee, D. S., Heikenfeld, J. & Birkhahn, R. Blue emission from Tm-doped GaN electroluminescent devices. *Appl. Phys. Lett.* **75**, 2184 (1999).
- Lozykowski, H. J., Jadwisieniczak, W. M. & Brown, I. Visible cathodoluminescence of GaN doped with Dy, Er, and Tm. *Appl. Phys. Lett.* **74**, 1129 (1999).
- Favennec, P. N., L'Haridon, H., Salvi, M., Moutonnet, D. & Le Guillou, Y. Luminescence of erbium implanted in various semiconductors: IV, III-V and II-VI materials. *Electron. Lett.* **25**, 718–719 (1989).
- Kenyon, A. J. Recent developments in rare-earth doped materials for optoelectronics. *Progress in Quantum Elect.* **26**, 225–284 (2002).
- Hömmrich, U. *et al.* Photoluminescence studies of rare earth (Er, Eu, Tm) *in situ* doped GaN. *Mat. Sc. Eng. B* **105**, 91–96 (2003).
- Hwang, J., Hashimoto, R., Saito, S. & Nunoue, S. Development of InGaN-based red LED grown on (0001) polar surface. *Appl. Phys. Express* **7**, 071003 (2014).
- Lozykowski, H. J., Jadwisieniczak, W. M., Han, J. & Brown, I. G. Luminescence properties of GaN and $\text{Al}_{0.14}\text{Ga}_{0.86}\text{N}/\text{GaN}$ superlattice doped with europium. *Appl. Phys. Lett.* **77**, 767 (2000).
- Sawahata, J., Bang, H., Seo, J. & Akimoto, K. Optical processes of red emission from Eu doped GaN. *Sc. Tech. Adv. Mat.* **6**, 644–648 (2005).
- Wakamatsu, R. *et al.* Luminescence Properties of Eu-Doped GaN Grown on GaN Substrate. *Jap. J. Appl. Phys.* **52**, 08JM03 (2013).
- de Boer, W. D. *et al.* Optical excitation and external photoluminescence quantum efficiency of Eu^{+3} in GaN. *Sci. Rep.* **4**, 5235 (2014).
- Wakamatsu, R., Timmerman, D., Lee, D., Koizumi, A. & Fujiwara, Y. Afterglow of Eu related emission in Eu-doped gallium nitride grown by organometallic vapor phase epitaxy. *J. Appl. Phys.* **116**, 043515 (2014).
- Heikenfeld, J., Garter, M., Lee, D. S., Birkhahn, R. & Steckl, A. J. Red light emission by photoluminescence and electroluminescence from Eu-doped GaN. *Appl. Phys. Lett.* **75**, 1189 (1999).

13. Kim, J. H. & Holloway, P. H. Room-temperature photoluminescence and electroluminescence properties of sputter grown gallium nitride doped with europium. *J. Appl. Phys.* **95**, 4787 (2004).
14. Park, J. H. & Steckl, A. J. Laser action in Eu-doped GaN thin-film cavity at room temperature. *Appl. Phys. Lett.* **85**, 4588 (2004).
15. Nishikawa, A., Kawasaki, T., Furukawa, N., Terai, Y. & Fujiwara, Y. Room-temperature red emission from a p-type/europium-doped/n-type gallium nitride light-emitting diode under current injection. *Appl. Phys. Express.* **2**, 071004 (2009).
16. Nishikawa, A., Kawasaki, T., Furukawa, N., Terai, Y. & Fujiwara, Y. Electroluminescence properties of Eu-doped GaN-based red light-emitting diode by OMVPE. *Phys. Stat. Sol. A* **207**, 1397–1399 (2010).
17. Nishikawa, A., Furukawa, N., Kawasaki, T., Terai, Y. & Fujiwara, Y. Improved luminescence properties of Eu-doped GaN light-emitting diodes grown by atmospheric-pressure organometallic vapor phase epitaxy. *Appl. Phys. Lett.* **97**, 051113 (2010).
18. Nishikawa, A., Furukawa, N., Kawasaki, T., Terai, Y. & Fujiwara, Y. Room-temperature red emission from light-emitting diodes with Eu-doped GaN grown by organometallic vapor phase epitaxy. *Optical Mat.* **33**, 1071–1074 (2011).
19. Sekiguchi, H. *et al.* Red light-emitting diodes with site-selective Eu-doped GaN active layer. *Jap. J. Appl. Phys.* **52**, 08JH01 (2013).
20. Ishii, M., Koizumi, A. & Fujiwara, Y. Nanoscale determinant to brighten up GaN:Eu red light-emitting diode: Local potential of Eu-defect complexes. *J. App. Phys.* **117**, (155307 (2015)).
21. Arai, T. *et al.* Enhanced excitation efficiency of Eu ions in Eu-doped GaN/AlGaIn multiple quantum well structures grown by organometallic vapor phase epitaxy. *J. Luminescence* **158**, 70–74 (2015).
22. Inaba, T. *et al.* Substantial enhancement of red emission intensity by embedding Eu-doped GaN into a microcavity. *AIP Adv.* **6**, 045105 (2016).
23. Zhu, W. *et al.* High-power Eu-doped GaN red LED based on a multilayer structure grown at lower temperatures by organometallic vapor phase epitaxy. *MRS Adv.* **67**, 159–164 (2017).
24. Okada, H. *et al.* Light emitting FET based-on spatially selective doping of Eu in AlGaIn/GaN HEMT. *Phys. Stat. Sol.* **6**, S631–S634 (2009).
25. Inaba, T., Mitchell, B., Koizumi, A. & Fujiwara, Y. Emission enhancement and its mechanism of Eu-doped GaN by strain engineering. *Optical Mat. Express* **7**, 1381–1387 (2017).
26. Fujiwara, Y. & Dierolf, V. Present understanding of Eu luminescent centers in Eu-doped GaN grown by organometallic vapor phase epitaxy. *Jap. J. Appl. Phys.* **53**, 05FA13 (2014).
27. Woodward, N. *et al.* Excitation of Eu³⁺ in gallium nitride epitaxial layers: Majority versus trap defect center. *Appl. Phys. Lett.* **98**, 011102 (2011).
28. Mitchell, B. *et al.* The role of donor-acceptor pairs in the excitation of Eu-ions in GaN:Eu epitaxial layers. *J. Appl. Phys.* **115**, 204501 (2014).
29. Masago, A., Fukushima, T., Sato, K. & Katayama-Yoshida, H. Efficient luminescent center by codoping (Eu,Mg,O) into GaN. *Appl. Phys. Express.* **7**, 071005 (2014).
30. Fragkos, I. E., Tan, C. K., Dierolf, V., Fujiwara, Y. & Tansu, N. Pathway towards high-efficiency Eu-doped GaN light-emitting diodes. *Sci. Rep.* **7**, 14648 (2017).
31. Nagarajan, R., Ishikawa, M., Fukushima, T., Geels, R. S. & Bowers, J. E. High speed quantum-well lasers and carrier transport effects. *IEEE J. Quantum. Electron.* **28**, 1990–2008 (1992).
32. Tansu, N. & Mawst, L. J. Current injection efficiency of 1300-nm InGaAsN quantum-well lasers. *J. Appl. Phys.* **97**, 054502 (2005).
33. Zhao, H. P., Liu, G. Y., Zhang, J., Arif, R. A. & Tansu, N. Analysis of internal quantum efficiency and current injection efficiency in nitride light-emitting diodes. *J. Disp. Technol.* **9**, 212–225 (2013).
34. Yeh, J. Y., Mawst, L. J. & Tansu, N. The Role of Carrier Transport on the Current Injection Efficiency of InGaAsN Quantum-WellLasers. *IEEE Photon. Technol. Lett.* **17**, 1779–1881 (2005).
35. Lee, C. W., Everitt, H. O., Lee, D. S., Steckl, A. J. & Zavada, J. M. Temperature dependence of energy transfer mechanisms in Eu-doped GaN. *J. Appl. Phys.* **95**, 7717 (2004).
36. Wang, J., Koizumi, A., Fujiwara, Y. & Jadwisienczak, W. M. Study of defects in GaN *in situ* doped with Eu³⁺ ion grown by OMVPE. *J. Elect. Mat.* **45**, 2001–2007 (2016).
37. Al Tahtamouni, T. M., Stachowicz, M., Li, J., Lin, J. Y. & Jiang, H. X. Dramatic enhancement of 1.54μm emission in Er doped GaN quantum well structures. *Appl. Phys. Lett.* **106**, 121106 (2015).
38. Al Tahtamouni, T. M., Li, J., Lin, J. Y. & Jiang, H. X. Current injection 1.54 μm light-emitting devices based on Er-doped GaN/AlGaIn multiple quantum wells. *Opt. Mat. Exp.* **6**, 3476–3481 (2016).
39. Amano, H., Sawaki, N., Akasaki, I. & Toyoda, Y. Metalorganic vapor phase epitaxial growth of a high quality GaN film using an AlN buffer layer. *Appl. Phys. Lett.* **48**, 353 (1986).
40. Hashimoto, T., Wu, F., Speck, J. S. & Nakamura, S. A GaN bulk crystal with improved structural quality grown by the ammonothermal method. *Nature Mater.* **6**, 568 (2007).
41. Nakamura, S. *In Situ* Monitoring of GaN growth using interference effects. *Jap. J. Appl. Phys.* **30**, 10A (1991).
42. Ee, Y. K. *et al.* Metalorganic vapor phase epitaxy of III-nitride light-emitting diodes on nano-patterned AGOG sapphire substrate by abbreviated growth mode. *IEEE J. Sel. Top. Quantum Electron.* **15**, 1066–1072 (2009).
43. Zavada, J. M. Impurity co-doping of gallium nitride materials for enhanced light emission. *ECS Trans.* **61**, 65–70 (2014).
44. Okamoto, K. *et al.* Surface plasmon-enhanced light emitters based on InGaIn quantum wells. *Nature Mater.* **3**, 601–605 (2004).
45. Okamoto, K. *et al.* Surface plasmon enhanced spontaneous emission rate of InGaIn/GaN quantum wells probed by time-resolved photoluminescence spectroscopy. *Appl. Phys. Lett.* **87**, 071102 (2005).
46. Neogi, A. *et al.* Enhancement of spontaneous emission in a quantum well by resonant surface plasmon coupling. *Phys. Rev. B* **66**, 153305 (2002).
47. Zhao, H. P., Zhang, J., Liu, G. Y. & Tansu, N. Surface plasmon dispersion engineering via double-metallic Au/Ag layers for III-nitride based light-emitting diodes. *Appl. Phys. Lett.* **98**, 151115 (2011).

Acknowledgements

This work was supported by US National Science Foundation (ECCS 1408051 and DMR 1505122), and the Daniel E. '39 and Patricia M. Smith Endowed Chair Professorship Fund.

Author Contributions

I.E.F. and N.T. contributed to the discussions, concept development, theoretical analysis, analysis of the results, and writing of the manuscript. V.D., and Y.F. contributed to the technical discussions, and analysis of the results. N.T. supervised the studies performed in the manuscript.

Additional Information

Competing Interests: The authors declare that they have no competing interests.

Publisher's note: Springer Nature remains neutral with regard to jurisdictional claims in published maps and institutional affiliations.



Open Access This article is licensed under a Creative Commons Attribution 4.0 International License, which permits use, sharing, adaptation, distribution and reproduction in any medium or format, as long as you give appropriate credit to the original author(s) and the source, provide a link to the Creative Commons license, and indicate if changes were made. The images or other third party material in this article are included in the article's Creative Commons license, unless indicated otherwise in a credit line to the material. If material is not included in the article's Creative Commons license and your intended use is not permitted by statutory regulation or exceeds the permitted use, you will need to obtain permission directly from the copyright holder. To view a copy of this license, visit <http://creativecommons.org/licenses/by/4.0/>.

© The Author(s) 2017